IOPscience

HOME | SEARCH | PACS & MSC | JOURNALS | ABOUT | CONTACT US

A micro optofluidic lens with short focal length

This article has been downloaded from IOPscience. Please scroll down to see the full text article.

2009 J. Micromech. Microeng. 19 085012

(http://iopscience.iop.org/0960-1317/19/8/085012)

The Table of Contents and more related content is available

Download details:
IP Address: 155.69.4.4
The article was downloaded on 14/07/2009 at 01:58

Please note that terms and conditions apply.

IOP PUBLISHING JOURNAL OF MICROMECHANICS AND MICROENGINEERING

J. Micromech. Microeng. **19** (2009) 085012 (6pp) doi:10.1088/0960-1317/19/8/085012

A micro optofluidic lens with short focal length

Chaolong Song, Nam-Trung Nguyen, Say-Hwa Tan and Anand Krishna Asundi

School of Mechanical and Aerospace Engineering, Nanyang Technological University, 50 Nanyang Avenue, Singapore 639798

E-mail: mntnguyen@ntu.edu.sg

Received 11 February 2009, in final form 15 May 2009
Published 13 July 2009
Online at stacks.iop.org/JMM/19/085012

Abstract

A micro optofluidic lens is formed by laminar streams of immiscible liquids with different refractive indices. This paper reports modelling and characterization for a new design of a micro optofluidic lens. The lens has a circular chamber allowing the formation of interfaces with a perfect arc shape. The inlet and the outlet of the lens chamber are placed with an offset to the chamber axis to achieve a radius of curvature smaller than the limiting chamber radius. A model mathematically predicts the relationship between the flow rate ratio and the curvature of the interface and the resulting focal length. The device was fabricated and tested with laser light guided by optical fibres. Experiments were carried out to verify the analytical model. Benzyl alcohol and ethylene glycol were used as optical media to form the lens. Due to the small radius of curvature, better focusing ability than the previous symmetric design was achieved. On-chip focusing with fibre-to-fibre transmission was demonstrated with this micro optofluidic lens.

1. Introduction

Recently, the field of optofluidics that combines optics and fluidics has attracted growing interest of the research community [1]. Integrating optofluidic components into a microfluidic system presents new potentials for lab-on-a-chip (LOC) devices. Wave guides [2], optical switch [3] and microring resonator laser [4] have been demonstrated to work on a microfluidic device. Lenses as important optical components have also been intensively investigated for on-chip integration and other applications. Several groups reported the fabrication and the characterization of polydimethylsiloxane (PDMS)-based optical lenses [5–7]. However, these solid-based lenses are not reconfigurable. Furthermore, the optical smoothness depends on the fabrication process. Tang *et al* [8] proposed the use of hydrodynamic spreading in a rectangular chamber to develop a reconfigurable fluidic lens, which can collimate and focus light on the plane of the microchannels. The device concept is based on a liquid flow at low Reynolds numbers. The core stream sandwiched by two cladding streams enters the circular chamber and then expands to develop the lens shape. The curvature of the interface of the lens and the focal length can be tuned by adjusting the flow rates of the cladding streams and the core stream. Due to the geometric limit of a rectangular lens chamber, the shape of the lens interface is not a perfect arc, especially when the interface approaches the wall of the chamber. The subsequent problem is the weak focusing ability as the result of the compromise between achieving large curvature of the interface and obtaining an arc shape around the paraxial region. The same design was later reported by Seow *et al* [9]. The rectangular designs in these previous works led to a flat interface near the optical axis. An arc-shape interface would allow a simple prediction of the aberration. The main advantage of an arc interface is that the spherical aberration can be minimized or neglected around the paraxial region. A plano-convex lens with its arc-shape interface towards the beam source can converge a parallel beam to a sharper focal spot or collimate a diverging beam to a parallel beam.

In a previous work, we proposed the use of a source and sink pair model to mathematically describe the fluidic aspect of an optofluidic lens [10]. In this optofluidic lens, the direction of the flow channel coincides with the axis of a circular chamber where the lens is hydrodynamically formed. This paper presents a new design with inlet and outlet channels placed with an offset to the axis of a circular chamber as

 © 2009 IOP Publishing Ltd Printed in the UK

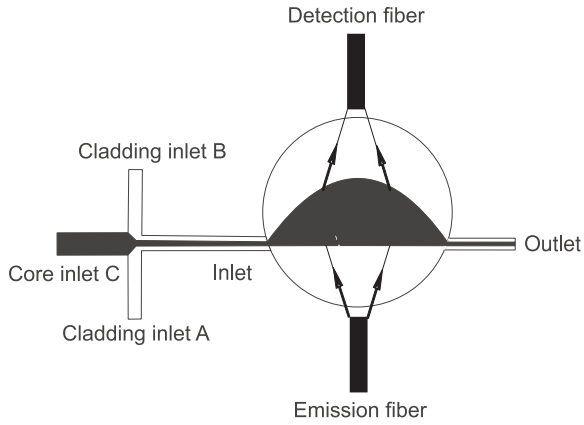

Figure 1. Hydrodynamic formation of optofluidic lens in a circular chamber with the inlet/outlet channel shifting. Optical fibres are aligned along the optical axis of the lens for testing its focusing ability.

illustrated in figure 1. The purpose of this design is to shift the inlet and outlet away from the centre of the circular chamber. With this measure, the curvature of the upper interface can overcome the restriction of the chamber geometry and achieve a maximum value. Therefore, this method promises to shorten the focal length and thus reinforce the focusing ability. In this paper, we first establish a model to describe the fluidic aspect of our new design and consequently derive the relationship between the flow rate ratio and the curvature of the interface. The interface of the lens is demonstrated to have a perfect arc shape. The experiment also verifies that our theory can mathematically pre-define the shape of the optofluidic lens. Finally, benzyl alcohol and ethylene glycol were used to form the lens and to test the tunability of its focal length; the focusing ability of the lens is also demonstrated.

2. Theory

In our design, the width of the channel is much smaller than the dimension of the chamber. So the entrance and exit of the circular chamber act approximately as a source and sink, respectively. Assuming that the sink is placed at (x_0, y_0), and the source is symmetrically located at $(-x_0, y_0)$, as illustrated in figure 2(*a*), the complex potential of this flow field can be written as

$$W = \phi + \mathrm{i}\psi = \ln \frac{(z + x_0 - \mathrm{i}y_0)\left(z + \frac{R^2}{x_0 + \mathrm{i}y_0}\right)}{(z - x_0 - \mathrm{i}y_0)\left(z + \frac{R^2}{-x_0 + \mathrm{i}y_0}\right)}, \tag{1}$$

where i is the imaginary unit and R is the radius of the lens chamber. The streamlines shown in figure 2(*b*) are the equipotential lines of the imaginary part of the complex potential W. In our previous work, we have demonstrated that the streamlines in a circularly bounded potential flow theoretically have a perfect arc shape [10].

According to the theory of potential flow, the first derivative of the complex potential with respect to z represents the velocity field $\overrightarrow{V} = (u, v)$. The real and imaginary parts of this first derivative represent the velocity components in the x-axis and y-axis, respectively. Differentiating W in

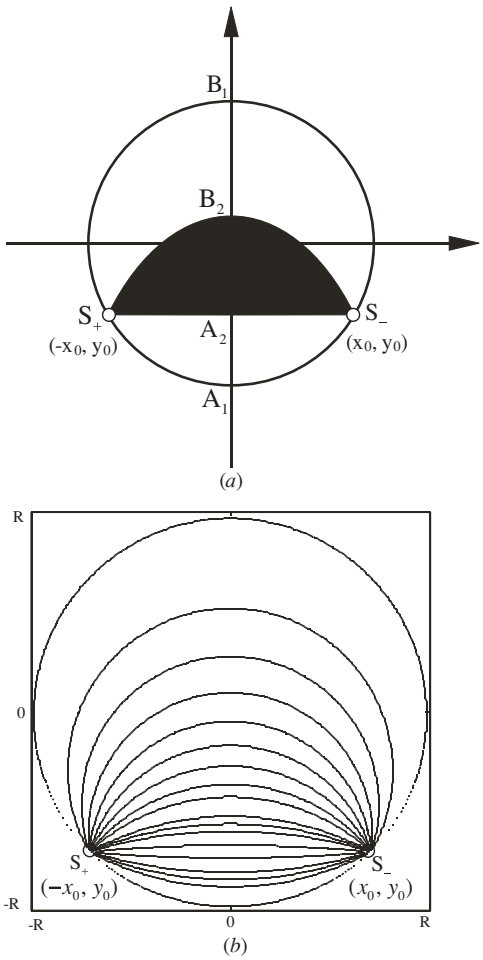

Figure 2. Mathematic model of the optofluidic lens: (*a*) interface positions and (*b*) streamlines of the source–sink pair in a circularly bounded domain with source and sink located at the circumference.

equation (1) with respect to z results in the velocity components, and the velocity distribution along the y-axis is as follows:

$$\begin{cases} u = \frac{4x_0}{y^2 - 2y_0 y + R^2} \\ v = 0. \end{cases} \tag{2}$$

The curvatures of the two interfaces determine the positions of A_2 and B_2 and therefore decide the flow rates for core and cladding flows, respectively:

$$\begin{cases} \phi_{\text{cladding B}} = \int_{B_2}^{B_1} u\,\mathrm{d}y = \int_{B_2}^{B_1} \frac{4x_0}{y^2 - 2y_0 y + R^2}\,\mathrm{d}y \\ = \frac{4x_0}{\sqrt{R^2 - y_0^2}}\left[\arctan\left(\frac{R - y_0}{\sqrt{R^2 - y_0^2}}\right) - \arctan\left(\frac{y_{B_2} - y_0}{\sqrt{R^2 - y_0^2}}\right)\right] \\ \phi_{\text{core}} = \int_{A_2}^{B_2} u\,\mathrm{d}y = \int_{A_2}^{B_2} \frac{4x_0}{y^2 - 2y_0 y + R^2}\,\mathrm{d}y \\ = \frac{4x_0}{\sqrt{R^2 - y_0^2}}\left[\arctan\left(\frac{y_{B_2} - y_0}{\sqrt{R^2 - y_0^2}}\right) - \arctan\left(\frac{y_{A_2} - y_0}{\sqrt{R^2 - y_0^2}}\right)\right] \\ \phi_{\text{cladding A}} = \int_{A_1}^{A_2} u\,\mathrm{d}y = \int_{A_1}^{A_2} \frac{4x_0}{y^2 - 2y_0 y + R^2}\,\mathrm{d}y \\ = \frac{4x_0}{\sqrt{R^2 - y_0^2}}\left[\arctan\left(\frac{y_{A_2} - y_0}{\sqrt{R^2 - y_0^2}}\right) - \arctan\left(\frac{-R - y_0}{\sqrt{R^2 - y_0^2}}\right)\right], \end{cases} \tag{3}$$

where $\phi_{\text{cladding A}}$, $\phi_{\text{cladding B}}$ and ϕ_{core} are the flow rates per unit depth of the cladding and the core streams. Equation (3) can basically be used to work out any corresponding flow rates of core/cladding streams with a required shape of lens. For

mathematical simplicity, we will consider a plano-convex lens and derive its relationship between the flow rate ratio and curvature of the interface. To further shorten the focal length of the optofluidic lens, we will also consider a lens developed by a two-phase flow as depicted in the inset in figure 3.

To achieve a plano-convex lens, the y-axis position of the interface $\overline{S_+A_2S_-}$ should be the same as that of the source and the sink, which is equal to y_0. Suppose that $y_0 = -0.5R$; we can get the relationship between the position of the upper interface $\overline{S_+B_2S_-}$ and the flow rate ratio by substituting $y_{A_2} = y_0$ into equation (3):

$$Q_{\text{plano-convex}} = \frac{\phi_{\text{core}}}{\phi_{\text{cladding B}}} = \frac{\alpha}{\pi/3 - \alpha} \tag{4}$$

with

$$\alpha = \arctan\left(\frac{y_{B_2} + 0.5R}{\sqrt{3}R/2}\right). \tag{5}$$

The position of the intersections between the interface and the y-axis is calculated as

$$y_{B_2} = y_0 + r - \sqrt{r^2 - x_0^2}, \tag{6}$$

where r is the radius of curvature of the upper interface $\overline{S_+B_2S_-}$ (figure 2(a)). Combining equations (4) and (6) results in the relation between the factor β and the radius of curvature R:

$$\alpha = \arctan\left(\frac{y_0 + r - \sqrt{r^2 - x_0^2} + 0.5R}{\sqrt{3}R/2}\right). \tag{7}$$

The focal length of the lens depends on the radius r of the interface curvature:

$$f = \frac{r}{n-1}, \tag{8}$$

where $n = n_{\text{core}}/n_{\text{cladding}}$, n_{core} and n_{cladding} are the relative refractive index and the indices of the core liquid and the cladding liquid, respectively. The focal length is denoted as f. Substituting equation (8) into equation (7) results in the relationship between the focal length and the factor α:

$$\alpha = \arctan\left(\frac{y_0 + f(n-1) - \sqrt{f^2(n-1)^2 - x_0^2} + 0.5R}{\sqrt{3}R/2}\right). \tag{9}$$

Figure 3(a) graphically shows the relationship between the flow rate ratio and the normalized focal length $f^* = f/R$ for different relative refractive indices.

In the case of matching refractive indices between the cladding liquid and the chamber material, the shortest focal length can be obtained by eliminating the lower cladding. The lower lens interface then has the same radius as the lens chamber. To model the lens developed by the two-phase flow, the flow rate ratio of the core to the upper cladding B can be written as

$$Q_{\text{two-phase}} = \frac{\phi_{\text{core}}}{\phi_{\text{cladding B}}} = \frac{\pi/6 + \beta}{\pi/3 - \beta} \tag{10}$$

with

$$\beta = \arctan\left(\frac{y_0 + r - \sqrt{r^2 - x_0^2} + 0.5R}{\sqrt{3}R/2}\right), \tag{11}$$

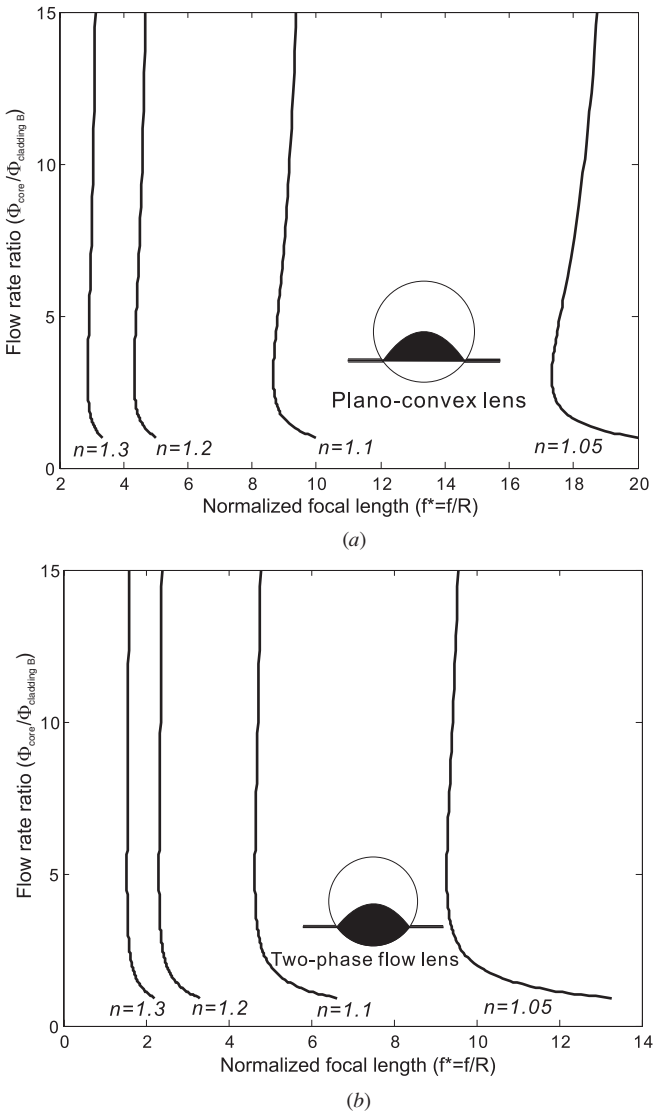

Figure 3. Relationships between the flow rate ratio and focal length (the dimension of the focal length is normalized by the radius of the circular chamber): (a) plano-convex lens and (b) two-phase lens.

where r is the tunable radius of the upper interface (figure 6). In this two-phase convex lens, the lower interface is fixed with a radius equal to that of the chamber wall R. Thus, the focal length can be formulated as

$$f = \frac{r \cdot R}{(n-1)(r+R)}. \tag{12}$$

Combining equations (10) and (12) results in the relationship between the factor β and the focal length of the two-phase convex lens as illustrated in figure 3(b):

$$\beta = \arctan\left(\frac{y_0 + \frac{f(n-1)R}{R - f(n-1)} - \sqrt{\left[\frac{f(n-1)R}{R-f(n-1)}\right]^2 - x_0^2} + 0.5R}{\sqrt{3}R/2}\right). \tag{13}$$

By shifting the inlet/outlet away from the centre axis of the chamber, the shape of the upper interface can overcome the restriction of the chamber geometry, and thus have a maximum curvature, which corresponds to the minimum focal length in

figure 3. Therefore, the focal length can be greatly shortened compared with the symmetric geometry in our previous work [10]. This shorter focal length promises that the light focusing can be achieved within the area of a chip, which will be demonstrated in our later experiment.

3. Experiment and discussion

The device for the validation experiments was fabricated in PDMS using the soft lithography technique. The design was printed on a transparency film with a resolution of 8000 dpi. The transparency mask was subsequently used for defining the negative mould of the lens in a 50 μm thick SU-8 layer. Using the SU-8 mould as a master, PDMS was mixed in a weight ratio of 10:1 and poured onto it. Thereafter, PDMS was placed in a vacuum for 2 h to remove the gas bubbles. After the degassing process, PDMS was heated at 80 °C for 2 h. PDMS was then peeled off from the master mould and 0.75 mm diameter access holes were punched using a puncher (Harris Uni-Core, World Precision Instruments Inc., FL). PDMS with the lens structure was subsequently bonded to another flat PDMS part after treating both surfaces with oxygen plasma. The bonded PDMS was then placed in the oven at 150 °C for a further 2 h to ensure good bonding between both surfaces. Needles with an inner diameter of 0.33 mm and an outer diameter 0.64 mm were press fitted into the access holes and worked as fluidic interconnects. With this technology, a circular lens chamber with a diameter of 1 mm and a height of 50 μm was realized. The width of the inlet and exit channels is 50 μm.

For the validation experiment, cladding liquid is de-ionized (DI) water mixed with w/w fluorescence dye (fluorescein disodium salt $C_{20}H_{10}Na_2O_5$, acid yellow 73 or C.I. 45350) and 3 μm red fluorescent particles (Duke Scientific Co.) were used to visualize the cladding liquid and its stream lines. The separated fluorescent bands of the fluorescent particles (540/610 nm) and of the dye (490/520 nm) allow easy imaging by switching the epi-fluorescent attachments on the microscope (Nikon EclipseTE 2000-S, Japan). DI water works as the core liquid. The liquids were kept in 5 ml glass syringes, which are driven by two syringe pumps (KDS230, KD Scientific Inc, USA) which allow any flow rate ratio needed. A sensitive CCD camera (HiSense MKII) attached to the microscope was used to capture the fluorescent images.

First, flow visualization with fluorescent particles verified that the streamlines in the circular chamber have a perfect arc shape, which is of great importance for designing the optofluidic lens. As mentioned above, red fluorescent particles are diluted in the two cladding flows that maintain the same flow rates as that of the core flow. A sufficiently long exposure time of 100 ms was chosen, within which a particle can travel from the inlet to the outlet of the circular chamber. In this way, the particles will leave streak lines on the image as illustrated in the inset of figure 4. Since the flow is laminar in our case, the streak lines of the particles correspond to the streamlines of the flow in the chamber. We extract a group of positions for each of the three paths shown in figure 4 and use an arc to fit each of them. The agreement between the extracted positions

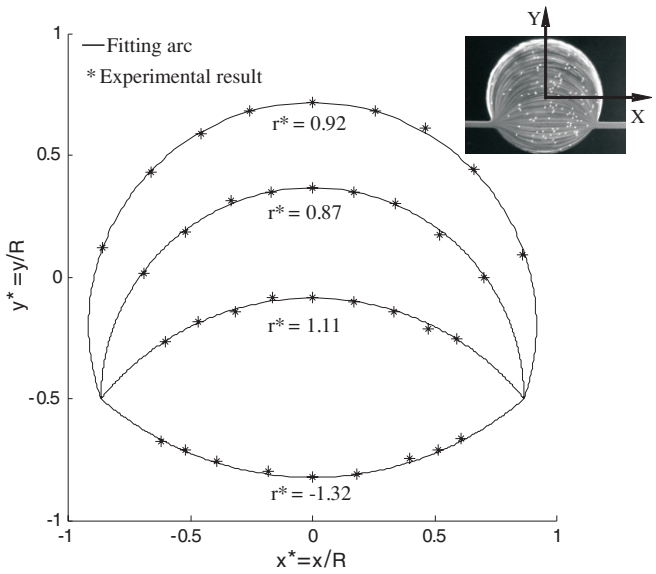

Figure 4. The streamlines of the flow in the circular chamber are extracted by tracing of fluorescent particles. The asterisks in the figure represent the experimental results and the lines are the fittings arcs (all dimensions are normalized by the radius of the lens chamber).

and fitting arcs confirms that the streamlines in the circular chamber have a perfect arc shape, which cannot be achieved with a rectangular chamber [8].

To verify the theory for predicting the relationship between the flow rate ratio and the curvature of the interface, blue light was used to excite the fluorescent dye dissolved in the cladding flows. The core flow with no fluorescent dye appears black on the image. The interface between the dark and bright regions was extracted; its curvature was also evaluated under different flow rate ratios between the core and cladding flows.

The measurement of the plano-convex design (figure 1) validates its mathematically predicted shape. In the experiment, the total flow rate was fixed at 2.4 mL h^{-1}, and the corresponding Reynolds number and Peclet number were 1.33 and 1333 respectively. The flow rate of cladding A was kept constant at 0.8 mL h^{-1}, whereas the flow rate ratio of the core to cladding B was tuned in a range from 0.33 to 11. Figure 5 shows the relationship between the flow rate ratio $Q_{\text{plano-convex}} = \phi_{\text{core}}/\phi_{\text{cladding B}}$ and the normalized curvature of upper interface R/r theoretically and experimentally. As the flow rate ratio increases, the upper interface becomes more curved. Its shape remains an arc during the tuning process even when the interface approaches the wall of the chamber. One point worth to mention here is the maximum curvature. According to equation (7), the curvature of the upper interface reaches its maximum value $R/x_0 = 1.15$, when the flow rate of core stream is thrice that of cladding B (the curvature of the wall of the circular chamber normalized by itself is equal to 1). This fact was verified by the experiment illustrated in figure 5. The enhancement of curvature due to the shift of the inlet and outlet makes shortening the focal length possible and therefore reinforces the focusing ability. For comparison, we calculate the theoretical curvature of the interface of a plano-convex lens developed in symmetric geometry reported earlier in [10]

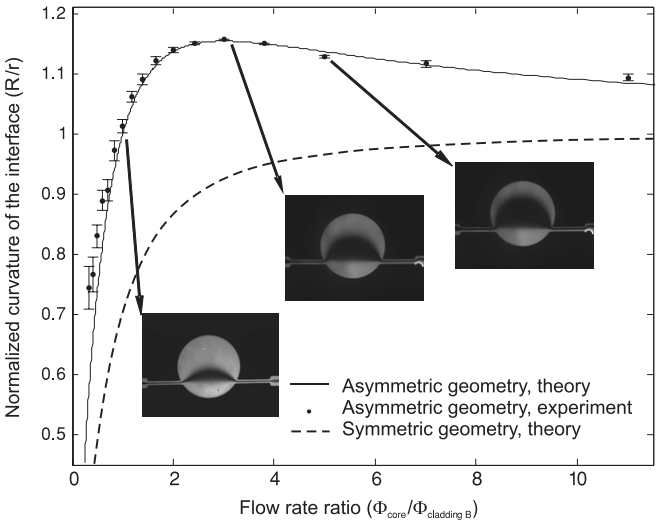

Figure 5. The relationship between the curvature of interface and the flow rate ratio. Asymmetric and symmetric cases are both illustrated and compared for developing a plano-convex lens. The insets illustrate the fluorescence images of the lenses in asymmetric geometry. The dimensions are normalized by the radius of the circular chamber. For experimental results in asymmetric geometry, the total flow rate was fixed at 2.4 mL h^{-1}, and the corresponding Reynolds number and Peclet number were 1.33 and 1333 respectively. The flow rate of lower cladding was kept at a constant 0.8 mL h^{-1}, whereas the flow rate ratio of the core to cladding B was tuned in a range from 0.33 to 11.

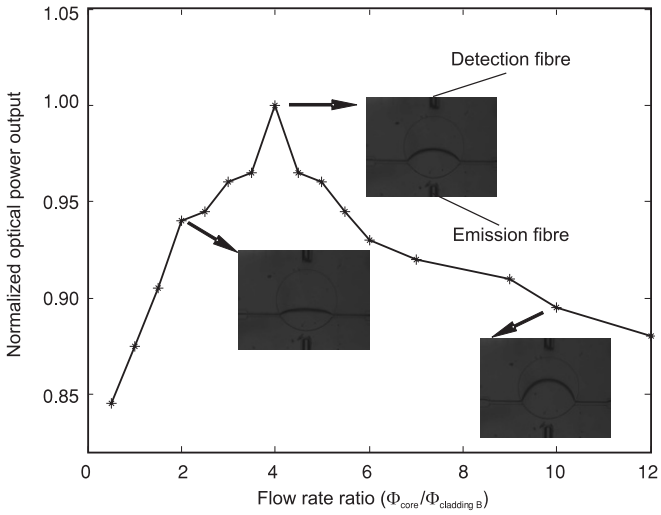

Figure 6. The variation of the signal output by changing the flow rate ratio. Emission and detection fibres are aligned and positioned along the optical axis of the optofluidic lens to test its focusing ability. The upper interface of the lens is tuned by changing the flow rate ratio of lower to upper streams, which results in a shifting of the focal point along the optical axis. The signal output is normalized by its maximum.

and depict it as the dotted line in figure 5. The limit of the curvature finally goes to 1, when the flow rate ratio becomes infinitely large.

To demonstrate the tunability of our lens, we used benzyl alcohol ($n = 1.538$) to shape the lens and converge the light beam, and ethylene glycol ($n = 1.429$) to match the refractive index of PDMS ($n = 1.412$). The same lens design was fabricated in PDMS but with a channel height of 150 μm to accommodate the optical fibres. The optical fibres (AFS105/125Y, THORLABS Inc.) have a core diameter of 105 μm, a clad diameter of 125 μm, a buffer diameter of 250 μm and a numerical aperture of NA = 0.22. For detecting the droplets, once the emission fibre is positioned and aligned to a laser source (laser diode, $\lambda = 635$ nm), the detection fibre is connected to an avalanche photodiode module (APD, C5460-01, Hamamtsu, Japan). The two-phase lens configuration (figure 3(*b*)) was used to get the shortest focal length possible. We blocked the inlet A (figure 1) and let the core stream take up one of the cladding streams. In this way, one of the lens interfaces is fixed with a curvature of the circular chamber; the other is tuned by changing the flow rate ratio of the lower (benzyl alcohol) to the upper (ethylene glycol) streams (figure 6). Because the refractive indices of ethylene glycol and PDMS almost match each other, the upper stream has a negligible impact on beam focusing. In the experiment, the light emitting and detection fibres were slotted into the guides fabricated in the same process as the lens chamber. The fibres are aligned and positioned along the optical axis of the lens. Figure 6 shows the experimental result of the variation of the output signal. By varying the flow rate ratio, the curvature of the upper interface can be changed and therefore tune the focal length of the optofluidic lens. As the flow rate ratio increases, the upper interface becomes more curved. This results in a shorter focal length. When the flow rate ratio of lower to upper streams reached a value of 4, the signal output achieves a maximum. At this maximum, the divergence of the focal spot created may match the NA of the fibre. Increasing the flow rate ratio further causes a drop in the output signal. In this experiment, the signal variation proves that this single optofluidic lens has a tunable focal length.

4. Conclusion

In conclusion, we proposed a new design to develop an optofluidic lens with very short focal length. The shape of the lens is tunable and can be mathematically predicted. As a result of the geometric advantage of the circular chamber, the interfaces of lens take on a perfect arc shape, which is of great importance in optical design. The shortest focal length can be achieved with the lower interface adopting the chamber curvature. Benzyl alcohol and ethylene glycol were used to form the lens and also demonstrate the on-chip focusing ability. Test results with optical fibres showed that the focal length can be tuned by adjusting the flow rate ratio. In the future works, we will design ray tracing chambers for determining the position of the focal point.

References

[1] Horowitz V R, Awschalom D D and Pennathur S 2008 Optofluidics: field or technique? *Lab Chip* **8** 1856–63
[2] Wolfe D B, Conroy R S, Garstecki P, Mayers B T, Fischbach M A, Paul K E, Prentiss M and Whitesides G M

2008 Dynamic control of liquid-core/liquid-cladding optical waveguides *Proc. Natl Acad. Sci.* **101** 12434–8

[3] Nguyen N-T, Kong T-F, Goh J-H and Low C L-N 2007 A micro optofluidic splitter and switch based on hydrodynamic spreading *J. Micromech. Microeng.* **17** 14613–2174

[4] Suter J D, Sun Y, Howard D J, Victor J A and Fan X 2008 PDMS embedded opto-fluidic microring resonator lasers *Opt. Express* **16** 10248–53

[5] Camou S, Fujita H and Fujii T 2003 PDMS 2D optical lens integrated with microfluidic channels: principle and characterization *Lab Chip* **3** 40–5

[6] Pang L, Levy U, Campbell K, Groisman A and Fainman Y 2005 Set of two orthogonal adaptive cylindrical lenses in a monolith elastomer device *Opt. Express* **13** 9003–13

[7] Yu H, Zhou G, Siong C F and Lee F 2008 Simple method for fabricating solid microlenses with different focal lengths *IEEE Photon. Technol. Lett.* **20** 1624–6

[8] Tang S K Y, Stan C A and Whitesides G M 2008 Dynamically reconfigurable liquid-core liquid-cladding lens in a microfluidic channel *Lab Chip* **8** 395–401

[9] Seow Y C, Liu A Q, Chin L K, Li X C, Huang H J, Cheng T H and Zhou X Q 2008 Different curvatures of tunable liquid microlens via the control of laminar flow rate *Appl. Phys. Lett.* **93** 084101

[10] Song C L, Nguyen N T, Tan S H and Asundi A 2009 Modelling and optimization of micro optofluidic lenses *Lab Chip* **9** 1178–84